1.1 DEVELOPMENT OF ADVANCED REDUCED ACTIVATION FERRITIC/MARTENSITIC STEELS -

L. Tan, X. Chen (Oak Ridge National Laboratory)

OBJECTIVE

Traditional reduced activation ferritic/martensitic (RAFM) steels suffer noticeable strength reduction at temperatures above ~500°C, which limits their high temperature applications. This project is to develop manufacturable and affordable advanced RAFM steel having an optimized alloy composition and thermomechanical treatment (TMT) to produce high density of stable nanoprecipitates for superior high temperature performance.

SUMMARY

The effect of different TMTs on microstructures has been characterized by electron backscattered diffraction (EBSD). The increased interweaving of the microstructures with refined local misorientation zones may be responsible for the improved ductility and Charpy impact resistance. A new RAFM steel has been designed to favor the formation of a high density of MC (M = metal) carbides. The preliminary result of optical images exhibited the presence of a large amount of precipitates in the matrix. Mechanical testing and detailed microstructural characterization of the new alloy will be conducted. Microstructural characterization of the high-dose Fe^{2+} ion irradiated TaC, TaN, and VN specimens has shown different evolutions of the particles as compared to evolution under low-dose irradiation.

PROGRESS AND STATUS

Introduction

Alloy TT1 in the normalized and tempered (N&T) condition has shown excellent yield and tensile strength but mediocre ductility at temperatures up to 800°C. To improve ductility, four types of TMT conditions, involving the application of warm-rolling (WR) and tempering, have been explored using Grade 92 that has a basic tempered martensitic microstructure similar to the TT1 alloy. The major composition difference from Grade 92 is the elimination of Mo, Nb and N and the alloying of Ta and Ti in alloy TT1 to reduce long-term alloy activation and manage the amount of MC precipitates. The best TMT condition, determined by tensile performance and Charpy impact resistance, has been selected and applied to the alloy. This report describes the effect of TMTs on microstructures and preliminary results of the alloy. Additionally, high-dose Fe^{2+} ion irradiated samples bearing TaC, TaN and VN nano-precipitates, respectively, have been characterized using TEM, which are to be briefly reported here.

Experimental Procedure

Computational thermodynamics was employed to optimize alloy composition of RAFM steels with an increased amount of MC-type precipitates. A new alloy, TT3M, has been fabricated using vacuum arc melting and drop casting, yielding a small experimental heat (~1 lb.). Part of the cast alloy was subjected to hot rolling followed by standard normalization (N) and tempering (T) heat treatment. One route of TMTs involved WR after normalization, followed by tempering, has been applied to alloy TT1.

Tensile testing was conducted using miniature specimens (type SS-3: 25.4 x 4.95 x 0.76 mm), machined along the rolling direction of the plate, at a nominal strain rate of 0.001 s^{-1}. Half-size Charpy specimens were extracted from the alloy plates in two orientations along the longitudinal (rolling) and transverse directions. The microstructures of the samples were characterized using optical microscopy, scanning electron microscopy (SEM), EBSD, and transmission electron microscopy (TEM). A FEI CM200 field-emission-gun TEM/STEM equipped with an EDAX energy dispersive X-ray spectroscopy (EDS) detector was primarily used to characterize the Fe^{2+}-irradiated samples. TEM specimens, perpendicular to the surfaces, were lifted out and thinned to electron-transparent using focused ion beam (FIB) on a Hitachi NB5000. Specimen thickness of the characterized regions was estimated using convergent beam electron diffraction (CBED) technique.

Results

The EBSD inverse pole figure (IPF) of the F2 TMT condition, namely N+WR+2T, of Grade 92 is shown in Figure 1, together with the IPF of the N&T condition for comparison. The orientation of the grain components is illustrated according to the color code in Figure 1. Regular prior-austenite grain structures and tempered martensite packets and blocks, which are clearly shown in the N&T condition, are significantly deformed by the TMT, leading to increased interweaving of the microstructures with refined local misorientations. The observed improvements in ductility and Charpy impact resistance of the samples in the TMT condition may be attributable to these changes. The F2 TMT has been applied to alloy TT1 and yielded slightly reduced yield and tensile strength but noticeably improved ductility as compared to the N&T condition of alloy TT1. However, the preliminary creep test at 650°C and 110 MPa exhibited a short creep life of 11.7 h with necking rupture close to the shoulder of type SS-3 specimen. The short creep life of the TMT sample may have resulted from misalignment and/or the specific features induced by the TMT. New creep tests will be conducted to eliminate the cause of misalignment.

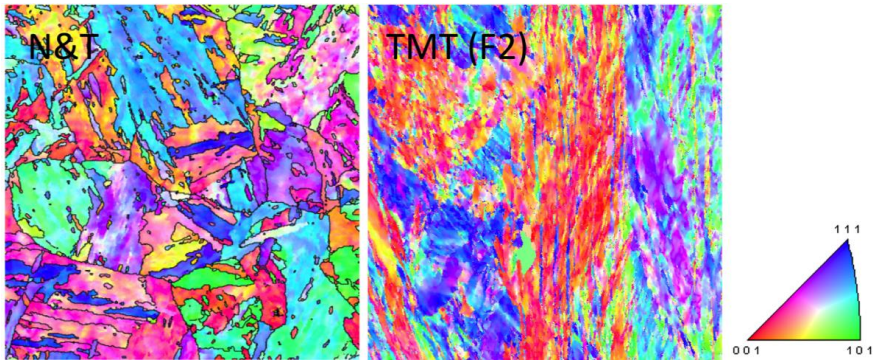

Figure 1. EBSD IPF maps (100×100 μm^2) of Grade 92 samples in the N&T and TMT conditions.

Based on the preliminary studies on the developed alloys TT1 and TT2, a new RAFM steel, TT3M, has been developed and fabricated. The major composition difference from alloy TT1 is the slightly increased amount of Mn and reduced V in alloy TT3M to optimize austenite temperature regime for improved efficiency of heat treatment. The optical micrograph of TT3M as compared to P92 is shown in Figure 2. The new alloy exhibits a large amount of precipitates in matrix, which is different from the observed precipitates in P92, primarily pinning lath/packet/block/prior-austenite boundaries. Further microstructural characterization will be conducted using SEM and TEM.

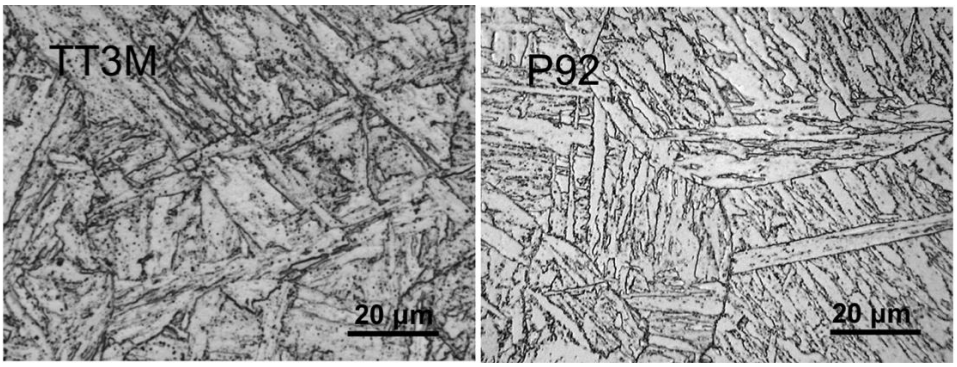

Figure 2. Optical micrographs comparison between alloy TT3M and P92.

The stability of TaN nanoprecipitates in a ferritic steel under Fe^{2+} ion irradiation to ~246 dpa at 500°C was characterized using TEM in dark-field (DF) mode. Figure 3 shows the DF image of TaN nanoprecipitates overlaid with the simulated irradiation dose depth profile using SRIM-2013 [3] using the parameters suggested in Ref. [4]. As compared to the low-dose irradiated sample that was reported earlier [1,2], the high-dose irradiation resulted in reduction in size and reduction in number density of TaN particles,

suggesting the dissolution of TaN particles. Unlike previously observed cavities in the TaC specimens subjected to the same high-dose irradiation, cavities were not observed in the TaN specimens. Characterization of the VN specimens has also completed. Statistical analysis of the collected images will be conducted.

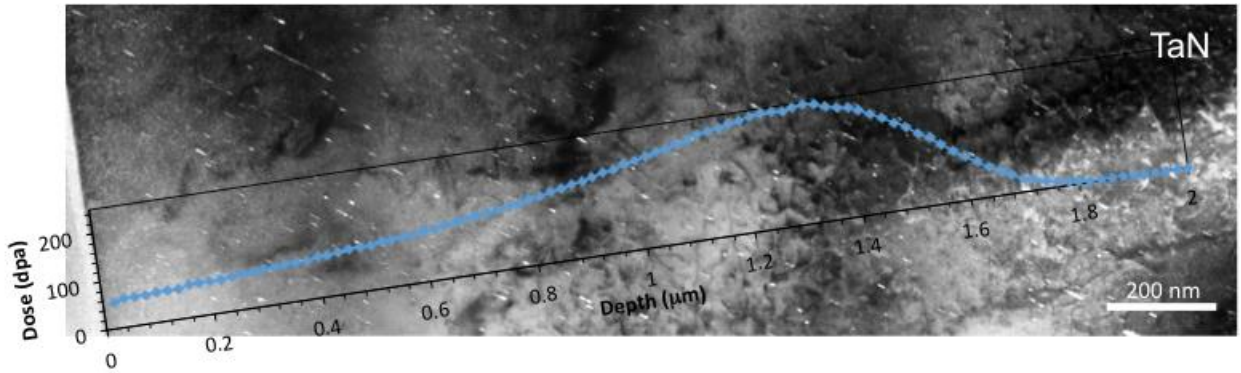

Figure 3. DF image showing the evolution of TaN nanoprecipitates as a function of the depth of Fe^{2+} ion irradiation at 500°C from surface on left, together with the overlaid SRIM simulation of irradiation dose depth profile.

References

[1] L. Tan, Y. Katoh, L.L. Snead, Stability of the strengthening nanoprecipitates in reduced activation ferritic steels under Fe^{2+} ion irradiation, Journal of Nuclear Materials 445 (2014) 104-110.

[2] L. Tan, T.S. Byun, Y. Katoh, L.L. Snead, Stability of MX-type strengthening nanoprecipitates in ferritic steels under thermal aging, stress and ion irradiation, Acta Materialia 71 (2014) 11-19.

[3] The Stopping and Range of Ions in Matter (SRIM) (http://www.srim.org).

[4] R.E. Stoller, M.B. Toloczko, G.S. Was, A.G. Certain, S. Dwaraknath, F.A. Garner, On the use of SRIM for computing radiation damage exposure, Nuclear Instruments and Methods in Physics Research B 310 (2013) 75-80.